ACS APPLIED MATERIALS & INTERFACES

Research Article

www.acsami.org

Enzyme-Labeled Pt@BSA Nanocomposite as a Facile Electrochemical Biosensing Interface for Sensitive Glucose Determination

Chenyi Hu,[†] Da-Peng Yang,*[,‡] Fengjuan Zhu,[†] Fengjing Jiang,[†] Shuiyun Shen,[†] and Junliang Zhang*[,†]

[†]Institute of Fuel Cell, Ministry of Education Key Laboratory of Power Machinery and Engineering, Shanghai Jiao Tong University, Shanghai 200240, China

[‡]Institute of Bioenergy and Bioprocess Technology, Laboratory for Biosensing, Chinese Academy of Sciences, Qingdao 266101, China

Supporting Information

ABSTRACT: Electrocatalytic reactions of glucose oxidation based on enzyme-labeled electrochemical biosensors demand a high enzymatic activity and fast electron transfer property to produce the amplified signal response. Through a "green" synthesis method, Pt@BSA nanocomposite was prepared as a biosensing interface for the first time. Herein we presented a convenient and effective glucose sensing matrix based on Pt@BSA nanocomposite along with the covalent adsorption of glucose oxidase (GOD). The electrocatalytic activity toward oxygen reduction was significantly enhanced due to the excellent bioactivity of anchored GOD and superior catalytic performance of interior platinum nanoparticles, which was gradually restrained with the addition of glucose. A sensitive glucose biosensor was then successfully developed upon the restrained oxygen reduction peak current. Differential pulse voltammetry (DPV) was employed to investigate the determination performance of the enzyme biosensor, resulting in a linear response range from 0.05 to 12.05 mM with an optimal detection limit of 0.015 mM. The as-proposed sensing technique revealed high selectivity against endogenous interfering species, satisfactory storage stability, acceptable durability, and favorable fabrication reproducibility with the RSD of 3.8%. During the practical application in human blood serum samples, this glucose biosensor obtained a good detection accuracy of analytical recoveries within 97.5 to 104.0%, providing an alternative scheme for glucose level assay in clinical application.

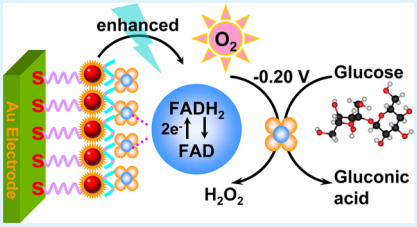

KEYWORDS: *Pt@BSA nanocomposite, biosensor, glucose oxidase (GOD), oxygen reduction, differential pulse voltammetry (DPV)*

1. INTRODUCTION

Diabetes mellitus is a metabolic illness characterized by hyperglycemia. It can bring about serious complications, such as strokes, kidney failure, blindness, etc.[1] Over the last few decades, much effort has been made to develop efficient techniques for glucose level assay on account of the clinical significance.[2] The existing detection methods including colorimetric determination,[3] electrochemiluminescence assay,[4] Raman spectrometry,[5] infrared spectroscopic analysis,[6] electrochemical approaches,[7] and so on, have been widely applied under diverse circumstances for different levels of requirements. A timely achievement of the accurate diagnosis of blood glucose level contributes to the prompt treatment and strict management of diabetes, and thus results in a greatly reduced possibility of complications caused by this disease. Therefore, designing a rapid, sensitive, selective, and stable protocol for monitoring of the blood glucose level is an urgent challenge in the current circumstances. Among the existent methods, electrochemical approaches, equipped with a series of outstanding features like ease of operation, lower cost, compatibility of miniaturization, rapid response, high sensitivity, and selectivity, have aroused significant concern from researchers for the purpose of developing a new generation of glucose sensor.[8−10] Normally, constructing an enzyme-labeled electrochemical glucose biosensor may possess some remarkable advantages over nonenzymatic glucose sensors, including the avoidance of endogenous interfering species at a low operating potential and much higher electrocatalytic activity toward analyte.[11,12] However, there still exist several defects in these enzyme biosensors, such as poor biostability and weak loading capacity of immobilized enzyme, unsatisfactory reproducibility, and deficient storage stability.[13] To resolve these problems, more and more researchers focus on developing novel nanomaterials as electrode sensing substrates, which have demonstrated lots of unusual advantages in electroanalysis such as improved catalytic reaction, more efficient electron transfer, increased surface area, good biocompability, and fine control over electrode microenvironment, etc.[14−17]

In the previous study, we synthesized a series of metal@protein (bovine serum albumin, BSA) nanocomposites via a "green" method.[18,19] In particular, the as-prepared Ag@BSA and Au@BSA microspheres showed excellent conductivity, biocompatibility, and stability, which were successfully employed as novel electrochemical interfaces for sensitive detection of H_2O_2,[20] retinal-binding protein,[21] KB cells[22] as

Received: December 18, 2013
Accepted: February 27, 2014
Published: February 27, 2014

   dx.doi.org/10.1021/am405841k | ACS Appl. Mater. Interfaces 2014, 6, 4170−4178

Scheme 1. Schematic Illustration of the Fabrication Process and Sensing Mechanism of the Pt@BSA-Based Electrochemical Glucose Biosensor

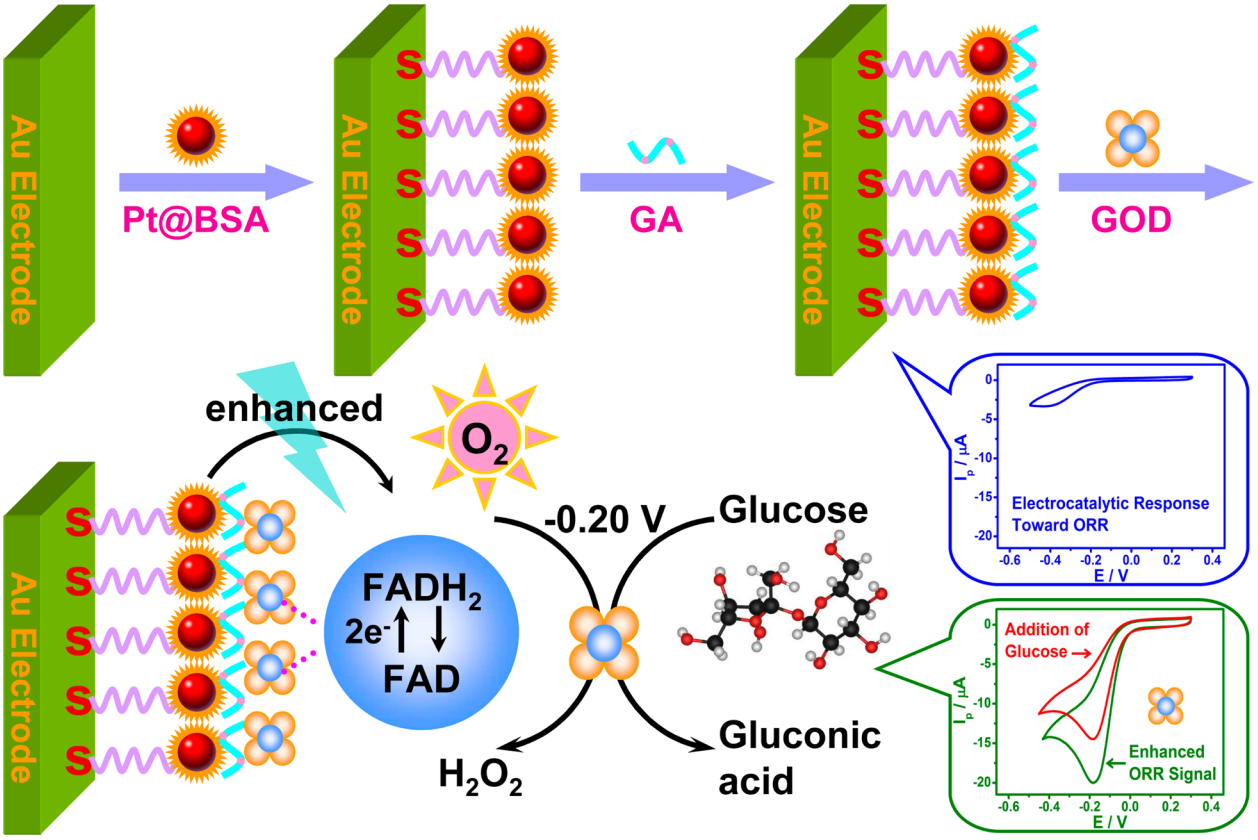

well as BXPC-3 cells.[23] Considering the importance of glucose determination in clinical assays, herein, we further developed an alternative "green nanomaterial"-Pt@BSA microsphere with enhanced electrocatalytic activity as electrochemical sensing matrix for glucose detection. When Pt@BSA composites were assembled onto the electrode surface, the reduction of dissolved oxygen was effectively facilitated due to the interior platinum nanoparticles (PtNPs) and greatly improved loading capacity of enzyme was achieved based on the outside BSA layer with a fairly large surface area. Moreover, the BSA layer could also serve as a protective film to maintain the good water permeability and bioactivity of anchored enzyme.[24,25] Glucose oxidase (GOD), a structurally rigid glycoprotein with a molecular mass of 150−180 kDa, performed as a homodimer composed of two identical polypeptide chains with two tightly bound flavin adenine dinucleotide (FAD) cofactors, which were deeply embedded in the protective protein shell and behaving as the active redox center.[26−28] The direct electron transfer between GOD and the electrode could be accelerated along with the covalent immobilization of GOD on Pt@BSA nanocomposite, revealing that the distance barrier of electron shuttle was effectively alleviated. The assembled sensing film could then electrocatalyze the reduction of dissolved oxygen and generate a great increase of reduction peak current. Upon the successive injection of β-D(+)-glucose, the GOD-based biosensor catalyzed the oxidation of glucose to gluconolactone in the presence of oxygen,[29] with the reduction peak current gradually decreased, making it suitable for glucose determination. Meanwhile, because of the satisfactory conductivity of Pt@BSA, the amplification of electrochemical signals could be realized on the sensing substrate, resulting in a better determination sensitivity.

It is probably fair to conclude that this research not only accomplishes the construction of a Pt@BSA-based glucose biosensor but also expands the application scope of BSA-based nanocomposites to the field of bioassay,[30] which may open up a new generation of biomedical approaches for clinical tests. Furthermore, this as-proposed sensing strategy also revealed qualified storage stability, excellent fabrication reproducibility, and good selectivity (excluding interferences from the potential electroactive substances), indicating a feasible strategy for glucose level assay in practical applications.

2. EXPERIMENTAL SECTION

Materials and Reagents. Chloroplatinic acid ($H_2PtCl_6·6H_2O$), glutaraldehyde solution 25% (GA), ascorbic acid (AA), uric acid (UA), 4-acetamidophenol (AP), and ethanol (CH_3CH_2OH) were acquired from Sinopharm Company (China). GOD (EC 1.1.3.4, type X-S, lyophilized powder, 100−250 units mg^{-1}, from *Aspergillus niger*), lyophilized 99% bovine serum albumin (BSA, molecular mass ∼66.4 KDa), and β-D(+)-glucose (≥99.5%) were purchased from Sigma-Aldrich Corporation. The 0.1 M phosphate buffer saline (PBS) solutions with various pH values were prepared by mixing stock standard solutions of Na_2HPO_4 and KH_2PO_4, and then adjusted to the required pH value with 0.1 M H_3PO_4 or NaOH. Ultrapure water obtained from a Millipore water purification system (Milli-Q, ≥18.2 MΩ) was used throughout the experiments. The glucose stock solutions were allowed for mutarotation by overnight storage at room temperature before use. The GOD solution with a certain concentration was prepared in pH 7.4 PBS and stored at 4 °C. Human blood serum samples were generously provided by Shanghai Ninth People's Hospital. Aqueous solutions of UA, AA, and AP were

dx.doi.org/10.1021/am405841k | ACS Appl. Mater. Interfaces 2014, 6, 4170−4178

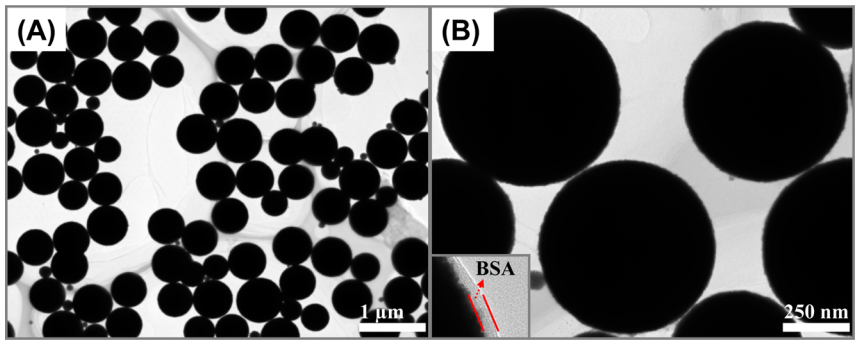

Figure 1. Typical TEM images of as-prepared Pt@BSA microspheres from (A) lower magnification to (B) higher magnification.

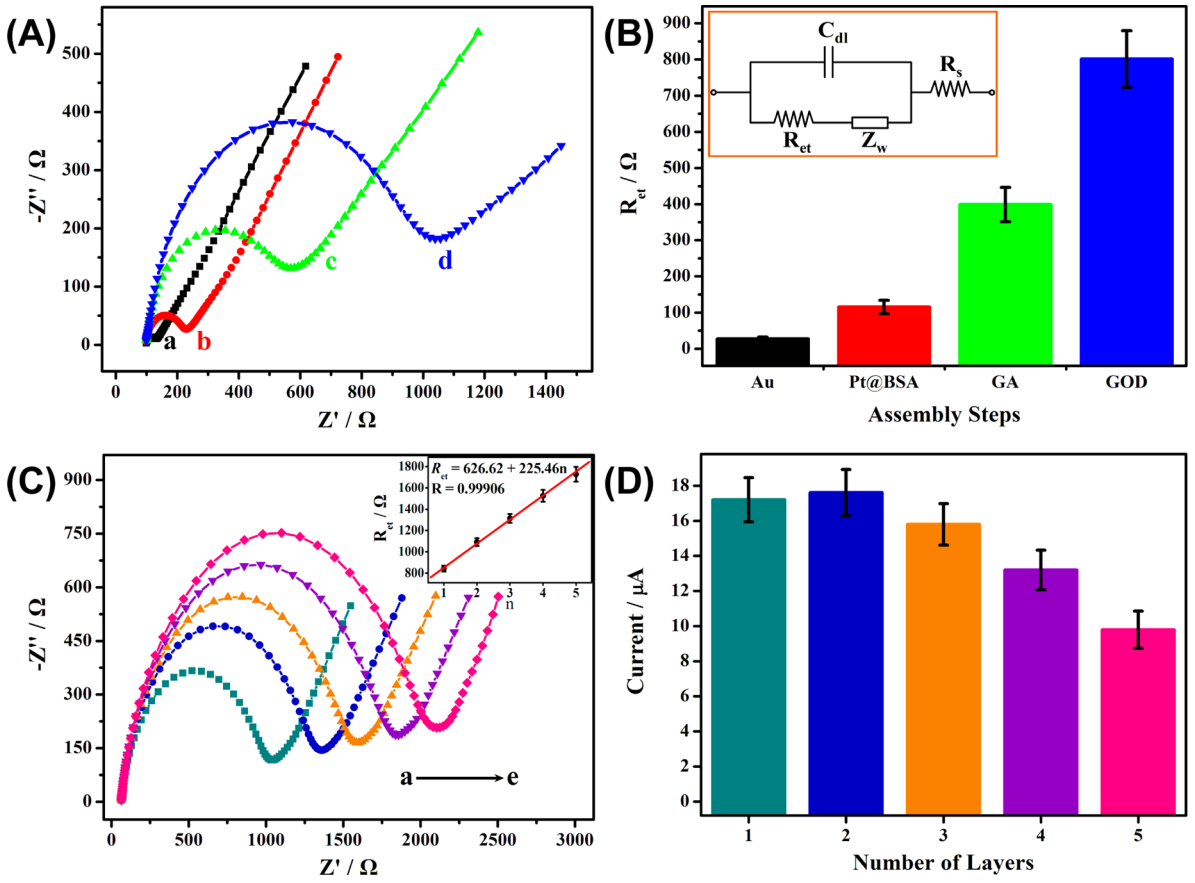

Figure 2. (A) Nyquist diagrams of electrochemical impedance spectra recorded from 1×10^{-2} to 1×10^{5} Hz in 0.1 M, pH 7.4 PBS containing $[Fe(CN)_6]^{3-}/[Fe(CN)_6]^{4-}$ (10 mM, 1:1) and 0.1 M KCl: (a) bare Au electrode upon electrochemical pretreatment, after (b) construction of Pt@BSA layer, (c) cross-linking reaction with GA, and (d) covalent conjugation of GOD. (B) The impedance results of assembly steps were fit into R_{et} values based on the equivalent circuit inset in part B. (C) EIS responses of $\{GOD/GA\}_n$/Pt@BSA-modified Au electrode with n increasing from 1 to 5. Inset: calibration curve of R_{et} values versus n. (D) CV responses of $\{GOD/GA\}_n$/Pt@BSA film electrode toward 1.50 mM glucose in 0.1 M, pH 7.4 PBS versus the bilayer number n. Error bars in B and D were the standard deviation of three replicate determinations.

instantly prepared using pH 7.4 PBS when they would be used. Unless otherwise noted, all the other reagents were of analytical grade and used as received without further purification.

Fabrication of the Modified Electrode and Assembly of GOD. The preparation of sensing film Pt@BSA microspheres was depicted in the Supporting Information. The detailed procedure for preparation of the Pt@BSA-based electrochemical glucose biosensor was graphically demonstrated in Scheme 1. Prior to chemical modification, the Au electrodes (2.0 mm in diameter) were polished sequentially with slurries of 1.0, 0.3, and 0.05 μm alumina powder to create a mirror shiny surface and followed by successive sonication in ethanol and ultrapure water, respectively. Then the polished electrodes were immersed into a mixture of piranha solution (98% H_2SO_4/30% H_2O_2, 3:1) for 3 min to debride possible residual contaminant, also rinsed with ethanol and ultrapure water, and dried under a stream of nitrogen. The experimental parameters were optimized in advance to obtain the best electrochemical response. Upon the electrochemical pretreatment, the Au electrode surface was dropped with 3 μL of Pt@BSA microspheres (2.0 mg mL^{-1}) to construct a biosensing interface and stored in the refrigerator at 4 °C for 2 h. After thoroughly rinsed with pH 7.4 PBS to remove physically adsorbed microspheres, the Pt@BSA-modified Au electrode was coated with 2.5 μL of freshly prepared 12.5% GA solution at ambient temperature for 1 h to achieve GOD attachment. Herein a high molar ratio of GA to Pt@BSA was employed to guarantee only one aldehyde group of GA reacting with amino groups of Pt@BSA.[31] Afterward, the electrode was rinsed with

pH 7.4 PBS again. Based on the above procedure, 3 μL of 15 mg mL^{-1} GOD solution (0.1 M, pH 7.4 PBS) was added onto the electrode surface and allowed to dry in the refrigerator at 4 °C overnight. Finally, GOD was covalently anchored onto the Pt@BSA microspheres through the formation of Schiff base structures, with the aid of GA, and used for studying the electrocatalytic oxidation of glucose. Before electrochemical experiments, the eventual GOD-immobilized electrodes were rinsed thoroughly with pH 7.4 PBS to wash away the unstably adsorbed biomolecules, which might lead to background interference, and preserved at 4 °C when not in use.

Apparatus and Electrochemical Measurements. The transmission electron microscopy (TEM) images were recorded on a JEOL JEM-2010 transmission electron microscope operating at an accelerating voltage of 200 kV and the scanning electron microscopy (SEM) images were obtained by a ZEISS-ULTRA 55 scanning electron microscope. Electrochemical measurements including electrochemical impedance spectroscopy (EIS), cyclic voltammetry (CV), and differential pulse voltammetry (DPV) were performed on a CHI 660E electrochemical workstation (CH instruments, China) with a conventional three-electrode cell comprised of a modified Au electrode as a working electrode, a platinum wire as an auxiliary electrode and a saturated calomel electrode (SCE) as reference. All measurements were carried out at the ambient temperature (25 ± 2 °C). Unless stated otherwise, CV and DPV experiments were conducted in air-saturated 0.1M, pH 7.4 PBS. The oxygen-free PBS buffer was prepared by bubbling high-purity nitrogen for 20 min to remove the dissolved oxygen. EIS experiments were performed in 0.1 M, pH 7.4 PBS containing $K_3Fe(CN)_6/K_4Fe(CN)_6$ (10 mM, 1:1) mixture and 0.1 M KCl as the supporting electrolyte, with a signal amplitude of 5 mV and a frequency range of 1×10^{-2} to 1×10^{5} Hz. ZsimpWin software version 3.10 was employed to fit the Nyquist diagrams into impedance results

3. RESULTS AND DISCUSSION

Characterization of Pt@BSA Microspheres and Assembly Process of Enzyme Biosensor. The construction of sensing substrate (Pt@BSA microspheres) plays a significant role in the electrocatalytic performance of the resulted biosensing device. For an electrochemical glucose enzyme transducer, Pt@BSA microspheres were quite effective for the controllable formation of hybrid sensing films through layer-by-layer (LBL) assembly from conjugated reactions based on the surface amino groups, and then greatly enhanced the electrocatalytic response attributed to the centric PtNPs. Figure 1 displayed the typical TEM images of the sensing substrate. The Pt@BSA microspheres showed spherical morphologies with an average size of 500 nm in diameter and a good monodispersity (Figure 1A), which contributed to developing a homogeneous film on the electrode surface. The energy dispersive spectroscopy (EDS) showed the dominant peaks of platinum (see Figure S1A in the Supporting Information), indicating of the major component of platinum. Higher magnification in Figure 1B demonstrated that a thin layer (BSA) behaved as the connections among the adjacent microspheres. In addition, the BSA layer wrapped outside the microsphere and core−shell structure of the nanocomposite could be explicitly confirmed owing to the image contrast. Herein, the BSA layer with excellent film-forming capability could not only improve the thermal stability and mechanical property of the sensing film but also act as a multifunctional interface to cross-link biomolecules (GOD) and maintain their bioactivity. A certain amount of nanoparticles aggregated around the microspheres were observed from the SEM image in the Supporting Information (Figure S1B), indicating that the formation of Pt@BSA microspheres was a self-assembly process.

As an available approach to monitor the interfacial properties of the modified electrodes, EIS has been generally employed to characterize the LBL assembly steps.[32,33] Figure 2A depicted that the electron transfer resistance (R_{et}) of the electrode at different stages altered gradually with the successive modification of Pt@BSA, GA, and GOD, which were measured at a formal potential of 0.21 V versus SCE ($[Fe(CN)_6]^{3-/4-}$ as the redox probe). For a bare Au electrode pretreated electrochemically, it showed a low R_{et} value of 27.04 Ω (curve a) because of the formation of rougher surface and oxygen-containing groups.[34] After Pt@BSA microspheres were stably immobilized onto the Au electrode surface through the strong effect of Au−S bonding,[35,36] R_{et} increased to the value of 115.3 Ω (curve b), revealing the satisfactory electrical conductivity with the introduction of sensing matrix. GOD was negatively charged in pH 7.4 PBS buffer,[37] making it suitably immobilized onto the positively charged Pt@BSA microspheres via electrostatic adsorption. To increase the conjugation efficiency of GOD, GA was utilized as a cross-linking agent to realize the covalent binding between Pt@BSA microspheres and GOD. Immediate and quantitative reaction with GA resulted in an increased R_{et} value of 398.7 Ω (curve c), probably on account of the fact that generated imines could hinder the penetration of the redox probe. Subsequently, GOD was conjugated onto the modified film through the "bridge effect" of GA and R_{et} increased to 801.1 Ω (curve d) because of the poor conductivity of GOD, which further blocked the redox probe. Moreover, the successful assembly of GOD could be also visually confirmed by SEM (see Figure S1C in the Supporting Information), exhibiting that GOD molecules overspread the microspheres which provided a large surface area for GOD loading and led to a compact interface. On the basis of the equivalent circuit model inset in Figure 2B, the impedance results were fitted into R_{et} values and illustrated by histogram.

Upon the stepwise growth of $\{GOD/GA\}_n$/Pt@BSA film, the sensing layer became thicker and then the R_{et} values increased linearly with n increasing from 1 to 5 (Figure 2C), testifying the LBL assembly process was well-behaved. As shown in Figure 2D, the peak current response in 0.1 M, pH 7.4 PBS presented an extremely slight increase with n up to 2 and decreased fleetly, which could be attributed to the blocked diffusion of glucose to the entrapped enzyme through the thicker film. Therefore, in consideration of convenient operation and favorable electrochemical response, $\{GOD/GA\}_1$/Pt@BSA film was adopted in this research.

Electrocatalytic Response of the LBL Assembled Film Toward Oxygen Reduction. CV experiments were conducted to investigate the catalytic behaviors of electroactive substances on the LBL assembled electrode surface (Figure 3). At the potential of around −0.32 V, an irreversible reduction peak of dissolved oxygen could be observed at the bare Au electrode in air-saturated 0.1 M, pH 7.4 PBS (curve a), which was calculated to be a two-electron oxygen reduction reaction (ORR) to generate hydrogen peroxide according to the Laviron equation.[38] This electrocatalysis process was distinctly promoted with the construction of Pt@BSA film (curve b), which was potentially owing to the internal PtNPs equipped with the property of improving ORR catalytic activity. Influenced by steric hindrance and kinetic solvent effect from GA, ORR was immediately blocked and gave rise to an ill-defined peak (curve c). However, after the formation of GOD/GA/Pt@BSA film, it showed a well-defined reduction peak at around −0.20 V (curve d) originating from the direct electron

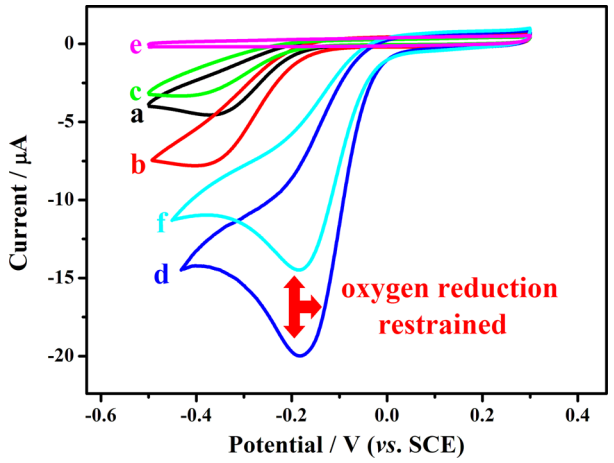

Figure 3. Cyclic voltammograms in air-saturated 0.1 M, pH 7.4 PBS at (a) an electrochemically pretreated bare Au electrode, (b) after formation of Pt@BSA layer, (c) after cross-linking reaction with GA, after covalent immobilization of GOD in the (d) presence and (e) absence of dissolved oxygen, and (f) with the addition of 6.55 mM glucose to air-saturated buffer. (scan rate: 50 mV s^{-1}).

transfer of GOD immobilized on the sensing matrix, which could effectively catalyze ORR. The reduction potential was even more positive than −0.32 V at the bare Au electrode and the peak shape was highly improved compared to curve a, suggesting the characteristic of electrocatalytic behavior toward ORR due to the presence of the hybrid sensing film. With the removal of dissolved oxygen, the above CV response disappeared under nitrogen-saturated atmosphere (curve e), mediately confirming the reduction of dissolved oxygen at the modified electrode which was catalyzed by the assembled GOD according to the following eqs 1 and 2

$$\mathrm{GOD(FAD) + 2e^- + 2H^+ \rightleftharpoons GOD(FADH_2)} \quad (1)$$

$$\mathrm{GOD(FADH_2) + O_2 \rightarrow GOD(FAD) + H_2O_2} \quad (2)$$

GOD molecule anchored on the surface of Pt@BSA microspheres displayed a rapid electron transfer at the electrode surface, undergoing a two-electron redox reaction, along with two-proton exchange. Its reduced form, GOD($FADH_2$), could catalyze ORR (2) and produce the oxidized form GOD(FAD), which was sequentially reduced (1). When a certain concentration of glucose was added into the air-saturated system, the reduction peak current apparently decreased (curve f) compared to curve d, expounding that electrocatalytic reaction was restrained due to the enzyme-catalyzed reaction as shown in eq 3 and consumption of oxygen.

$$\mathrm{Glucose + GOD(FAD) \rightarrow Gluconolactone + GOD(FADH_2)} \quad (3)$$

The reduction peak current decreased correspondingly with the increasing glucose concentration, developing an available technique for quantitative determination of glucose. The impact of scan rates on the cathodic and anodic peaks of GOD/GA/Pt@BSA was depicted in Figure S2 (see the Supporting Information). Both the cathodic and anodic peak currents increased proportionally with the scan rates within 10 to 400 mV s^{-1} (inset), which was the feature of a surface-controlled process. In general, the enzyme activity of GOD anchored on Pt@BSA microspheres was maintained and the direct electron transfer of GOD was realized at the LBL-modified electrode surface.

Optimization of Experimental Conditions for Glucose Sensing. To achieve prominent analytical performance of the fabricated biosensor, we took into account several interrelated parameters including the concentration of Pt@BSA, the concentration of GOD, experimental temperature, and pH value of the electrolyte solution. Pt@BSA, acting as the sensing substrate, is one of the most important factors influencing the detection sensitivity as well as enhancing the electrocatalytic activity. The effect of different concentrations of Pt@BSA ranging from 0.5 to 3.0 mg mL^{-1} on the electrochemical response was investigated by CV measurements in Figure 4A and a maximum CV peak current was obtained at 2.0 mg mL^{-1} owing to the optimal electron transfer rate, which was consequently applied for constructing the sensing interface. In addition, the detection performance of the enzyme biosensor is associated with the concentration of the GOD solution dropped on the electrode surface during the preparation of the ultimate GOD/GA/Pt@BSA film. Among the examined concentration range, CV response increased with the increasing GOD concentration and then reached a stable plateau at 15 mg mL^{-1} (Figure 4B), declaring that the GOD loading capacity of the assembled film was saturated and excess GOD from higher concentrations would be eliminated upon the rinsing procedure. With the purpose of enhancing the electrocatalytic activity, 15 mg mL^{-1} of GOD was selected for enzyme modification. Moreover, providing an appropriate testing environment by exploring a reasonable experimental temperature can be beneficial to maximizing the enzymatic activity of GOD and studying the thermostability of the proposed sensing approach. As shown in Figure 4C, the anchored GOD was treated at various temperatures ranging from 15 to 60 °C and a best enzymatic activity was acquired at around 25 °C, which was thus chosen as the optimum experimental temperature. The enzymatic activity remained relatively stable below 40 °C and maintained over 75% at 50 °C, exhibiting a good thermostability of the biosensor, and this should be attributed to the BSA layer acting as a protector of enzyme. Meanwhile, a sharp decrease in the enzymatic activity was observed at 60 °C because of the inactivation of GOD beyond the high temperature limit. The response signal of the glucose sensor also depends on the bioactivity of anchored GOD, which is closely related to pH value of the electrolyte solution. Figure 4D displayed the diverse CV peak currents of the biosensor toward 1.50 mM glucose with increasing the pH value from 4.4 to 10.4 and the maximum CV response was achieved at pH 7.4. At higher pH values, the response gradually decreased because of the enzyme denaturation and the steep loss of proton, which was crucial during the redox process of GOD(FAD). Therefore, the subsequent glucose determination was carried out in pH 7.4 PBS buffer to retain the top catalysis efficiency of GOD. Furthermore, it led to a negative shift in both cathodic (E_{pc}) and anodic (E_{pa}) peak potentials, thereby the formal potential ($E^{o\prime} = (E_{pc} + E_{pa})/2$) decreased linearly with the increasing pH value (inset in Figure 4D), with a slope of −52.3 mV pH^{-1} (R^2=0.997). This slope got close to the theoretical value of −58.6 mV pH^{-1} at 25 °C, demonstrating that two protons and two electrons participated in the electron transfer process.[39]

Quantitative Determination of Glucose via DPV. Under the optimal experimental conditions, an electrochemical glucose biosensor was developed on basis of the high

dx.doi.org/10.1021/am405841k | ACS Appl. Mater. Interfaces 2014, 6, 4170−4178

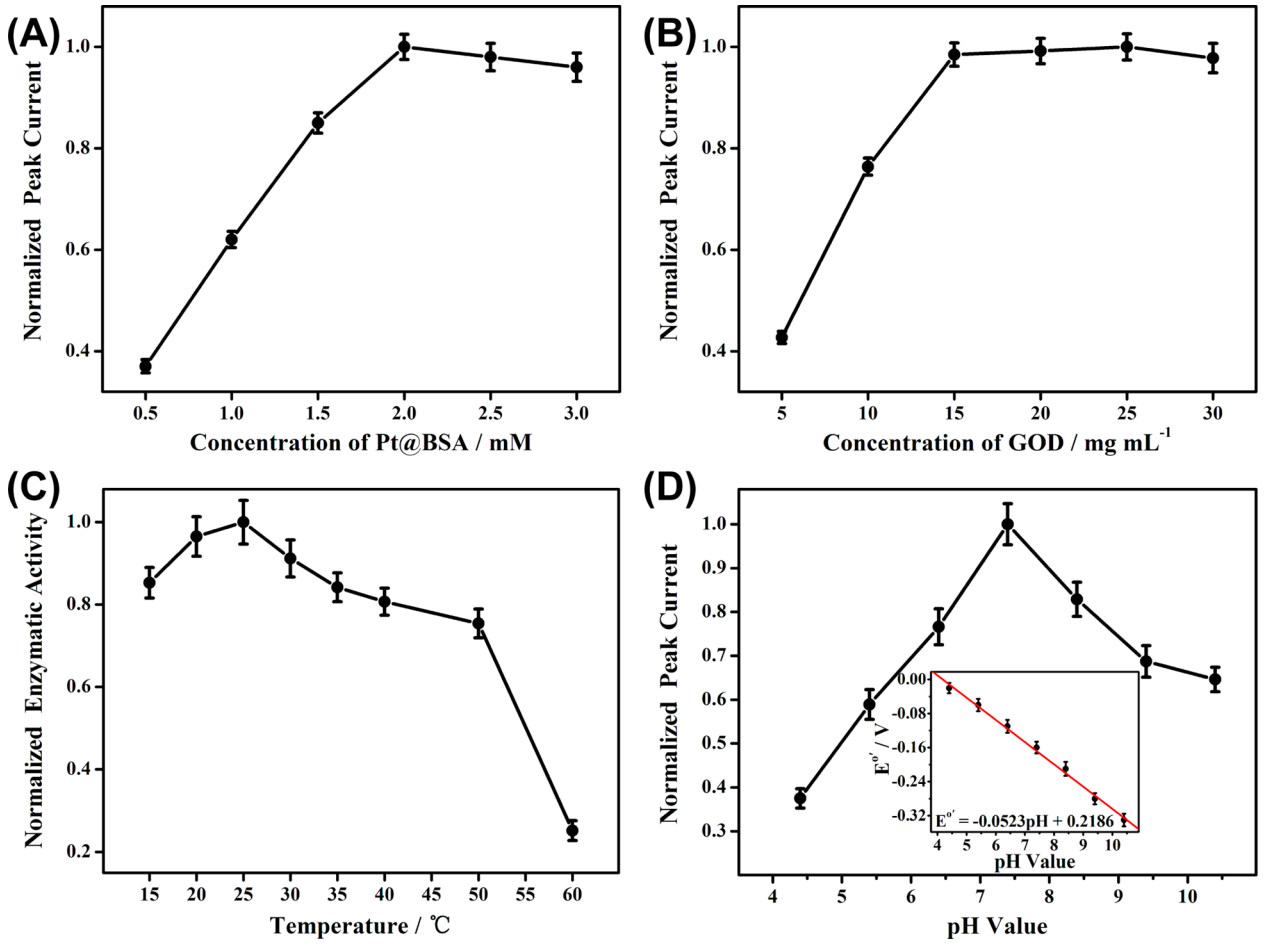

Figure 4. Effects of (A) concentration of Pt@BSA microspheres for construction of sensing substrate, (B) concentration of GOD for improvement of electrocatalytic activity, (C) experimental temperature, and (D) pH value of the electrolyte solution for glucose level assay on CV response at the modified Au electrodes in air-saturated 0.1 M PBS. Inset in part D: the dependence of formal potential ($E^{o\prime}$) as a function of pH value. All of the error bars were the standard deviation of five replicate determinations.

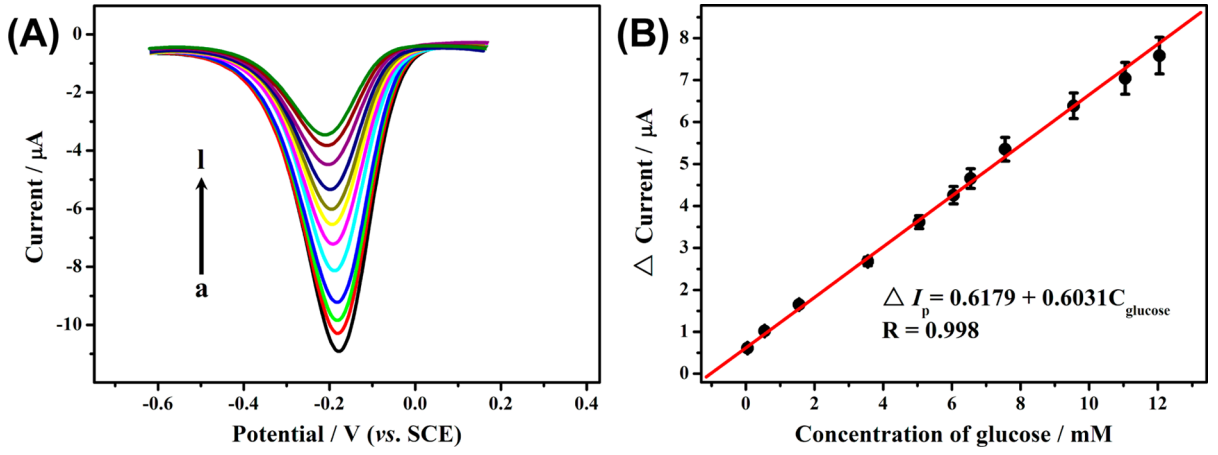

Figure 5. (A) Differential pulse voltammograms of GOD/GA/Pt@BSA-modified Au electrode in air-saturated 0.1 M, pH 7.4 PBS buffer (under the optimized conditions) with the glucose concentration increased from a to l (0.05, 0.55, 1.55, 3.55, 5.05, 6.05, 6.55, 7.55, 9.55, 11.05, 12.05 mM glucose injection, respectively). (B) Calibration curve of DPV amperometric biosensor for glucose determination at a pulse amplitude of 50 mV and a pulse width of 50 ms. Error bars were the standard deviation of three replicate measurements.

electrocatalytic activity of the sensing film toward oxygen reduction. Figure 5A showed the DPV measurements of the GOD/GA/Pt@BSA-modified electrodes in air-saturated 0.1 M, pH 7.4 PBS upon the injection of glucose with various concentrations. Due to the consumption of dissolved oxygen, the peak current originated from oxygen reduction at −0.20 V decreased linearly with increasing the glucose concentration from 0.05 to 12.05 mM. Moreover, a slight negative shift of the reduction peak potential was observed, which was probably attributed to the rapid augment of oxygen consumption with

dx.doi.org/10.1021/am405841k | ACS Appl. Mater. Interfaces 2014, 6, 4170−4178

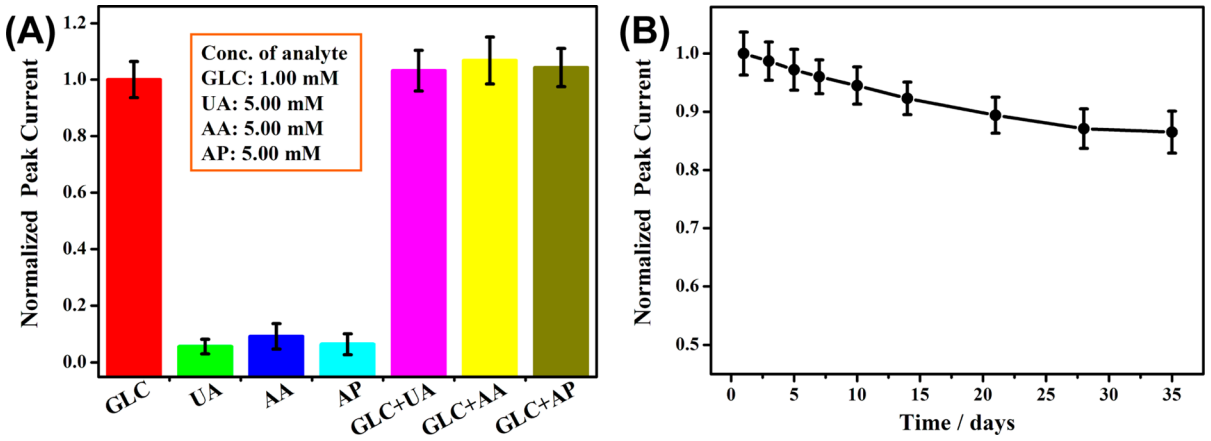

Figure 6. (A) Normalized electrocatalytic peak current changes of GOD/GA/Pt@BSA-modified Au electrode with the respective addition of 1.00 mM glucose (GLC), 5.00 mM UA, 5.00 mM AA, 5.00 mM AP, and mixed analytes by DPV measurements in air-saturated 0.1M, pH 7.4 PBS. (B) Normalized DPV peak current of as-fabricated glucose biosensor toward the oxidation of 1.50 mM glucose in air-saturated 0.1 M, pH 7.4 PBS during the storage period from 1 to 35 days. Error bars in A and B were the standard deviation of three replicate determinations.

added glucose content, accordingly leading to a systematic shift in potential drop. Figure 5B displayed the corresponding calibration plot of the background-subtracted DPV peak current versus the glucose concentration with a correlation coefficient of 0.998. The linear regression equation could be depicted as ΔI_p (μA) = 0.6179 + 0.6031$C_{glucose}$ (mM), with a detection limit of 0.015 mM at a signal-to-noise (S/N) ratio of 3. The sensitivity (the obtained linear slope divided by the electrode area) was evaluated to be 19.2 μA mM^{-1} cm^{-2}, which may be potentially enhanced by arranging {GOD/GA}n/Pt@BSA film into nanoelectrode arrays.[40−42] As shown in Figure S3 in the Supporting Information, amperometric response reached 95% of the steady state value after the addition of glucose within ~5s, which was similar to or shorter than those obtained at hybrid nanostructure (~3 s)[17] and multiwalled carbon nanotubes (~8 s).[38] It was worth noting that the upper limit of the glucose detection range was far beyond the normal physiological level of 3−8 mM, indicating that the proposed technique was feasible for glucose level assay in practical application. The obtained dynamic detection range in this work listed in Table S1 in the Supporting Information was comparable with or better than those previously reported results as 0.08−12 mM at the GOD/graphene/chitosan-modified electrode,[43] 0.01−1.11 mM at the GOD/PMB@$SiO_{2(nano)}$-modified electrode,[44] 2−14 mM at the GOD/graphene/PFIL-modified electrode,[45] 0.1−10 mM at the GOD/graphene-modified electrode,[46] 0.02−1.02 mM at the GOD/CNx-MWNT-modified electrode,[47] and 0.1−14 mM at the GOD-yeast$_{(nafion)}$/MWCNT-modified electrode.[48] Furthermore, we compared this biosensing performance with the electron-conducting hydrogels[49−52] and PtNPs-based nanocomposites,[53−56] revealing a possibility of improving performance by combining with these techniques. In general, this glucose sensing technique was superior to some conventional biosensors attributed to the favorable conductivity of Pt@BSA microspheres, enhanced electrocatalytic activity toward ORR, and maximized enzymatic activity of GOD, thus resulting in an amplification of electrochemical signals.

Evaluation of the Glucose Sensing Technique. The property to exclude the potential interference from commonly coexisted electroactive substances in the mimetic physiological environment is an important indicator for glucose biosensing. The effects of endogenous interfering species on DPV response were studied at the designed protocol. As shown in Figure 6A, the DPV current decrease caused by 5.00 mM UA, AA, and AP occupied only 5.6, 9.2, and 6.4% of which originated from 1.00 mM glucose, respectively, in the air-saturated 0.1 M, pH 7.4 PBS. By adding these interferences to the glucose analyte, no evident increase in the reduction peak current change was found compared to the current signal for 1.00 mM glucose, declaring that hardly any interference generated from those interfering species at a 5-fold excess because of the low operating potential. Consequently, the high selectivity of this sensing technique could be confirmed.

The practical application of the as-proposed biosensing approach in human blood serum samples was investigated by adopting the standard addition method. The serum samples obtained from the hospitalized patients were properly diluted by pH 7.4 PBS buffer in advance. In 10 mL of the diluted serum sample, the concentration of glucose was measured based on the calibration equation and the actual concentration could be obtained by multiplying the dilution ratio. The recovery experiments were carried out by adding 10 μL of 1.00 and 2.00 M glucose to 10 mL of real sample, which produced the analytical recoveries from 97.5 to 104.0% with the relative standard deviations (RSD) within 4.7% (listed in Table 1), demonstrating the good accuracy of glucose determination in real samples.

The storage stability of the GOD/GA/Pt@BSA-modified electrode was evaluated at intervals by DPV measurements toward 1.50 mM glucose and the electrode was stored in 0.1 M,

Table 1. Determination of Glucose in Human Blood Serum Samples

sample no.	sample found (mM)	glucose added (mM)	glucose found[a] (mM)	relative deviation (%)	recovery (%)
1	2.17	1.00	3.28	2.9	103.5
2	3.34	1.00	4.23	3.7	97.5
3	4.65	1.00	5.81	2.8	102.8
4	4.96	2.00	7.14	4.0	102.6
5	5.20	2.00	7.49	4.2	104.0
6	6.78	2.00	8.66	4.7	98.6

[a]The average value of five duplicate determinations for each sample by the GOD/GA/Pt@BSA-modified Au electrode.

pH 7.4 PBS under 4 °C when not in use. No distinct decrease in the response to glucose oxidation was observed after the storage of a week. Besides, it still remained about 86.5% of the initial current response after five weeks (shown in Figure 6B), revealing the satisfactory stability of as-prepared biosensor which could efficiently maintain the bioactivity of GOD. Normalized data were defined as the peak current of *n*th day divided by the peak current of the first day. The reproducibility of this biosensing approach was investigated by eight successive determinations toward 1.50 mM glucose and resulted in an RSD of 4.2%, showing a good intra-assay precision. Upon fifty sequential scans, 92.6% of its initial signal response was retained, exhibiting an acceptable durability and operation stability. Furthermore, six independently prepared electrodes from the batch were employed to estimate the interassay reproducibility with the obtained RSD of 3.8%, confirming the excellent fabrication reproducibility of this sensing strategy.

CONCLUSIONS

In summary, we demonstrated an efficient biosensing technique for rapid and sensitive determination of glucose based on the direct electrochemistry of GOD covalently anchored on Pt@BSA nanocomposite by virtue of glutaraldehyde, which undergone a two-proton participated two-electron redox process. Under an environmentally friendly synthesis route, Pt@BSA microspheres were expediently prepared and provided with some advantageous properties such as favorable biocompatibility, high recyclability, fast electron transfer rate, and enhanced electrocatalytic activity toward ORR. The restrained effect of glucose on the electrocatalytic behavior toward the reduction of dissolved oxygen resulted in the development of an efficient electrochemical biosensor for glucose level assay, possessing a satisfactory analytical performance with wide detection range, low detection limit, high selectivity, acceptable stability, and superior fabrication reproducibility. In addition, the proposed sensing strategy achieved a good accuracy of the practical application in real serum samples, providing a potential possibility for further investigation in clinical tests. Besides glucose sensing, it is considered that this enzyme-labeled technique can be also adjusted for some specific biological and physiological sensing requirements with deeper development, such as novel detection devices for high-density lipoprotein cholesterol (HDL-ch), lactate, choline, acetylcholine, and hypoxanthine.

ASSOCIATED CONTENT

Supporting Information

Additional information as noted in text. This material is available free of charge via the Internet at http://pubs.acs.org.

AUTHOR INFORMATION

Corresponding Authors

*E-mail: junliang.zhang@sjtu.edu.cn. Tel: 86-21-34207439. Fax: 86-21-34206249.

*E-mail: yangdp@qibebt.ac.cn.

Notes

The authors declare no competing financial interest.

ACKNOWLEDGMENTS

This work was supported by National Natural Science Foundation of China (Grant 21373135).

REFERENCES

(1) Alberti, K. G. M. M.; Zimmet, P. Definition, Diagnosis and Classification of Diabetes Mellitus and Its Complications. Part 1: Diagnosis and Classification of Diabetes Mellitus. Provisional Report of a WHO Consultation. *Diabetic Med.* **1998**, *15*, 539−553.

(2) Gochman, N.; Schmitz, J. M. Application of a New Peroxide Indicator Reaction to the Specific, Automated Determination of Glucose with Glucose Oxidase. *Clin. Chem.* **1972**, *18*, 943−950.

(3) Su, L.; Feng, J.; Zhou, X. M.; Ren, C. L.; Li, H. H.; Chen, X. G. Colorimetric Detection of Urine Glucose Based $ZnFe_2O_4$ Magnetic Nanoparticles. *Anal. Chem.* **2012**, *84*, 5753−5758.

(4) Chen, X. M.; Cai, Z. M.; Lin, Z. J.; Jia, T. T.; Liu, H. Z.; Jiang, Y. Q.; Chen, X. A Novel Non-Enzymatic Ecl Sensor for Glucose Using Palladium Nanoparticles Supported on Functional Carbon Nanotubes. *Biosens. Bioelectron.* **2009**, *24*, 3475−3480.

(5) Yuen, J. M.; Shah, N. C.; Walsh, J. T., Jr.; Glucksberg, M. R.; Van Duyne, R. P. Transcutaneous Glucose Sensing by Surface-Enhanced Spatially Offset Raman Spectroscopy in a Rat Model. *Anal. Chem.* **2010**, *82*, 8382−8385.

(6) Karoui, R.; Downey, G.; Blecker, C. Mid-Infrared Spectroscopy Coupled with Chemometrics: A Tool for the Analysis of Intact Food Systems and the Exploration of Their Molecular Structure-Quality Relationships - A Review. *Chem. Rev.* **2010**, *110*, 6144−6168.

(7) Liu, Y.; Wang, M.; Zhao, F.; Xu, Z.; Dong, S. The Direct Electron Transfer of Glucose Oxidase and Glucose Biosensor Based on Carbon Nanotubes/Chitosan Matrix. *Biosens. Bioelectron.* **2005**, *21*, 984−988.

(8) Wang, J. Electrochemical Glucose Biosensors. *Chem. Rev.* **2008**, *108*, 814−825.

(9) Wang, J. Carbon-Nanotube Based Electrochemical Biosensors: A Review. *Electroanaysis* **2005**, *17*, 7−14.

(10) Cao, X.; Wang, N.; Jia, S.; Shao, Y. Detection of Glucose Based on Bimetallic PtCu Nanochains Modified Electrodes. *Anal. Chem.* **2013**, *85*, 5040−5046.

(11) Luo, X.-L.; Xu, J.-J.; Du, Y.; Chen, H.-Y. A Glucose Biosensor Based on Chitosan−glucose Oxidase−gold Nanoparticles Biocomposite Formed by One-Step Electrodeposition. *Anal. Biochem.* **2004**, *334*, 284−289.

(12) Cai, C.; Chen, J. Direct Electron Transfer of Glucose Oxidase Promoted by Carbon Nanotubes. *Anal. Biochem.* **2004**, *332*, 75−83.

(13) Urban, G.; Jobst, G.; Kohl, F.; Jachimowicz, A.; Olcaytug, F.; Tilado, O.; Goiser, P.; Nauer, G.; Pittner, F.; Schalkhammer, T.; Mann-Buxbaum, E. Miniaturized Thin-Film Biosensors Using Covalently Immobilized Glucose Oxidase. *Biosens. Bioelectron.* **1991**, *6*, 555−562.

(14) Wang, J. Nanomaterial-Based Amplified Transduction of Biomolecular Interactions. *Small* **2005**, *1*, 1036−1043.

(15) Wang, J. Nanomaterial-Based Electrochemical Biosensors. *Analyst* **2005**, *130*, 421−426.

(16) Yang, W.; Ratinac, K. R.; Ringer, S. P.; Thordarson, P.; Gooding, J. J.; Braet, F. Carbon Nanomaterials in Biosensors: Should You Use Nanotubes or Graphene? *Angew. Chem., Int. Ed.* **2010**, *49*, 2114−2138.

(17) Meng, L.; Jin, J.; Yang, G.; Lu, T.; Zhang, H.; Cai, C. Nonenzymatic Electrochemical Detection of Glucose Based on Palladium−Single-Walled Carbon Nanotube Hybrid Nanostructures. *Anal. Chem.* **2009**, *81*, 7271−7280.

(18) Huang, P.; Yang, D.-P.; Zhang, C.; Lin, J.; He, M.; Bao, L.; Cui, D. Protein-Directed One-Pot Synthesis of Ag Microspheres with Good Biocompatibility and Enhancement of Radiation Effects on Gastric Cancer Cells. *Nanoscale* **2011**, *3*, 3623−3626.

(19) Wang, X.; Yang, D.-P.; Huang, P.; Li, M.; Li, C.; Chen, D.; Cui, D. Hierarchically Assembled Au Microspheres and Sea Urchin-Like Architectures: Formation Mechanism and SERS Study. *Nanoscale* **2012**, *4*, 7766−7772.

(20) Liu, Q.; Zhang, T.; Yu, L.; Jia, N.; Yang, D.-P. 3D Nanoporous Ag@BSA Composite Microspheres As Hydrogen Peroxide Sensors. *Analyst* **2013**, *138*, 5559−5562.

(21) Hu, C.; Yang, D. P.; Xu, K.; Cao, H.; Wu, B.; Cui, D.; Jia, N. Ag@BSA Core/Shell Microspheres As an Electrochemical Interface

for Sensitive Detection of Urinary Retinal-Binding Protein. *Anal. Chem.* **2012**, *84*, 10324−10331.
(22) Hu, C.; Yang, D.-P.; Wang, Z.; Huang, P.; Wang, X.; Chen, D.; Cui, D.; Yang, M.; Jia, N. Bio-mimetically Synthesized Ag@BSA Microspheres As a Novel Electrochemical Biosensing Interface for Sensitive Detection of Tumor Cells. *Biosens. Bioelectron.* **2013**, *41*, 656−662.
(23) Hu, C.; Yang, D.-P.; Wang, Z.; Yu, L.; Zhang, J.; Jia, N. Improved EIS Performance of an Electrochemical Cytosensor Using Three-Dimensional Architecture Au@ BSA As Sensing Layer. *Anal. Chem.* **2013**, *85*, 5200−5206.
(24) Ben-Knaz, R.; Avnir, D. Bioactive Enzyme−Metal Composites: The Entrapment of Acid Phosphatase within Gold and Silver. *Biomaterials* **2009**, *30*, 1263−1267.
(25) Tang, B.; Cao, L.; Xu, K.; Zhuo, L.; Ge, J.; Li, Q.; Yu, L. A New Nanobiosensor for Glucose with High Sensitivity and Selectivity in Serum Based on Fluorescence Resonance Energy Transfer (FRET) between CdTe Quantum Dots and Au Nanoparticles. *Chem.—Eur. J.* **2008**, *14*, 3637−3644.
(26) Huang, Y.; Zhang, W.; Xiao, H.; Li, G. An Electrochemical Investigation of Glucose Oxidase at a CdS Nanoparticles Modified Electrode. *Biosens. Bioelectron.* **2005**, *21*, 817−821.
(27) Jia, W. Z.; Wang, K.; Xia, X.-H. Elimination of Electrochemical Interferences in Glucose Biosensors. *TrAC, Trends Anal. Chem.* **2010**, *29*, 306−318.
(28) Wu, H.; Wang, J.; Kang, X.; Wang, C.; Wang, D.; Liu, J.; Aksay, I. A.; Lin, Y. Glucose Biosensor Based on Immobilization of Glucose Oxidase in Platinum Nanoparticles/Graphene/Chitosan Nanocomposite Film. *Talanta* **2009**, *80*, 403−406.
(29) Kadish, A. H.; Litle, R. L.; Sternberg, J. C. A New and Rapid Method for the Determination of Glucose by Measurement of Rate of Oxygen Consumption. *Clin. Chem.* **1968**, *14*, 2116−2131.
(30) Chen, A.; Holt-Hindle, P. Platinum-Based Nanostructured Materials: Synthesis, Properties, and Applications. *Chem. Rev.* **2010**, *110*, 3767−3804.
(31) Tan, Y.; Deng, W.; Ge, B.; Xie, Q.; Huang, J.; Yao, S. Biofuel Cell and Phenolic Biosensor Based on Acid-Resistant Laccase−Glutaraldehyde Functionalized Chitosan−Multiwalled Carbon Nanotubes Nanocomposite Film. *Biosens. Bioelectron.* **2009**, *24*, 2225−2231.
(32) Cui, R.; Liu, C.; Shen, J.; Gao, D.; Zhu, J. J.; Chen, H. Y. Gold Nanoparticle−Colloidal Carbon Nanosphere Hybrid Material: Preparation, Characterization, and Application for an Amplified Electrochemical Immunoassay. *Adv. Funct. Mater.* **2008**, *18*, 2197−2204.
(33) Suni, I. I. Impedance Methods for Electrochemical Sensors Using Nanomaterials. *TrAC, Trends Anal. Chem.* **2008**, *27*, 604−611.
(34) Hao, C.; Yan, F.; Ding, L.; Xue, Y.; Ju, H. A Self-Assembled Monolayer Based Electrochemical Immunosensor for Detection of Leukemia K562A cells. *Electrochem. Commun.* **2007**, *9*, 1359−1364.
(35) Rindzevicius, T.; Alaverdyan, Y.; Dahlin, A.; Höök, F.; Sutherland, D. S.; Käll, M. Plasmonic Sensing Characteristics of Single Nanometric Holes. *Nano Lett.* **2005**, *5*, 2335−2339.
(36) Lee, M. H.; Yang, Z.; Lim, C. W.; Lee, Y. H.; Dongbang, S.; Kang, C.; Kim, J. S. Disulfide-Cleavage-Triggered Chemosensors and Their Biological Applications. *Chem. Rev.* **2013**, *113*, 5071−5109.
(37) Lvov, Y.; Ariga, K.; Ichinose, I.; Kunitake, T. Assembly of Multicomponent Protein Films by Means of Electrostatic Layer-by-Layer Adsorption. *J. Am. Chem. Soc.* **1995**, *117*, 6117−6123.
(38) Zhao, H.; Ju, H. Multilayer Membranes for Glucose Biosensing via Layer-by-Layer Assembly of Multiwall Carbon Nanotubes and Glucose Oxidase. *Anal. Biochem.* **2006**, *350*, 138−144.
(39) Costentin, C. Electrochemical Approach to the Mechanistic Study of Proton-Coupled Electron Transfer. *Chem. Rev.* **2008**, *108*, 2145−2179.
(40) Lin, Y.; Lu, F.; Tu, Y.; Ren, Z. Glucose Biosensors Based on Carbon Nanotube Nanoelectrode Ensembles. *Nano Lett.* **2004**, *4*, 191−195.
(41) Claussen, J. C.; Wickner, M. M.; Fisher, T. S.; Porterfield, D. M. Transforming the Fabrication and Biofunctionalization of Gold Nanoelectrode Arrays into Versatile Electrochemical Glucose Biosensors. *ACS Appl. Mater. Interfaces* **2011**, *3*, 1765−1770.
(42) Claussen, J. C.; Hengenius, J. B.; Wickner, M. M.; Fisher, T. S.; Umulis, D. M.; Porterfield, D. M. Effects of Carbon Nanotube-Tethered Nanosphere Density on Amperometric Biosensing: Simulation and Experiment. *J. Phys. Chem. C* **2011**, *115*, 20896−20904.
(43) Kang, X.; Wang, J.; Wu, H.; Aksay, I. A.; Liu, J.; Lin, Y. Glucose Oxidase−Graphene−Chitosan Modified Electrode for Direct Electrochemistry and Glucose Sensing. *Biosens. Bioelectron.* **2009**, *25*, 901−905.
(44) Xiao, X.; Zhou, B.; Zhu, L.; Xu, L.; Tan, L.; Tang, H.; Zhang, Y.; Xie, Q.; Yao, S. A Reagentless Glucose Biosensor Based on Direct Electrochemistry of Glucose Oxidase Immobilized on Poly(Methylene Blue) Doped Silica Nanocomposites. *Sens. Actuators, B* **2012**, *165*, 126−132.
(45) Shan, C.; Yang, H.; Song, J.; Han, D.; Ivaska, A.; Niu, L. Direct Electrochemistry of Glucose Oxidase and Biosensing for Glucose Based on Graphene. *Anal. Chem.* **2009**, *81*, 2378−2382.
(46) Wu, P.; Shao, Q.; Hu, Y.; Jin, J.; Yin, Y.; Zhang, H.; Cai, C. Direct Electrochemistry of Glucose Oxidase Assembled on Graphene and Application to Glucose Detection. *Electrochim. Acta* **2010**, *55*, 8606−8614.
(47) Deng, S.; Jian, G.; Lei, J.; Hu, Z.; Ju, H. A Glucose Biosensor Based on Direct Electrochemistry of Glucose Oxidase Immobilized on Nitrogen-Doped Carbon Nanotubes. *Biosens. Bioelectron.* **2009**, *25*, 373−377.
(48) Wang, H.; Lang, Q.; Li, L.; Liang, B.; Tang, X.; Mascini, M.; Liu, A. Yeast Surface Displaying Glucose Oxidase as Whole-Cell Biocatalyst: Construction, Characterization, and Its Electrochemical Glucose Sensing Application. *Anal. Chem.* **2013**, *45*, 19−24.
(49) Zhai, D.; Liu, B.; Shi, Y.; Pan, L.; Wang, Y.; Li, W.; Zhang, R.; Yu, G. Highly Sensitive Glucose Sensor Based on Pt Nanoparticle/Polyaniline Hydrogel Heterostructures. *ACS Nano* **2013**, *7*, 3540−3546.
(50) Pan, L.; Yu, G.; Zhai, D.; Lee, H. R.; Zhao, W.; Liu, N.; Wang, H.; Tee, B. C.-K.; Shi, Y.; Cui, Y.; Bao, Z. Hierarchical Nanostructured Conducting Polymer Hydrogel with High Electrochemical Activity. *Proc. Natl. Acad. Sci. U.S.A.* **2012**, *109*, 9287−9292.
(51) Heller, A. Electron-Conducting Redox Hydrogels: Design, Characteristics and Synthesis. *Curr. Opin. Chem. Biol.* **2006**, *10*, 664−672.
(52) Åsberg, P.; Inganäs, O. Hydrogels of a Conducting Conjugated Polymer As 3-D Enzyme Electrode. *Biosens. Bioelectron.* **2003**, *19*, 199−207.
(53) Claussen, J. C.; Kumar, A.; Jaroch, D. B.; Khawaja, M. H.; Hibbard, A. B.; Porterfield, D. M.; Fisher, T. S. Nanostructuring Platinum Nanoparticles on Multilayered Graphene Petal Nanosheets for Electrochemical Biosensing. *Adv. Funct. Mater.* **2012**, *22*, 3399−3405.
(54) Hrapovic, S.; Liu, Y.; Male, K. B.; Luong, J. H. T. Electrochemical Biosensing Platforms Using Platinum Nanoparticles and Carbon Nanotubes. *Anal. Chem.* **2004**, *76*, 1083−1088.
(55) Claussen, J. C.; Franklin, A. D.; Haque, A. ul; Porterfield, D. M.; Fisher, T. S. Electrochemical Biosensor of Nanocube-Augmented Carbon Nanotube Networks. *ACS Nano* **2009**, *3*, 37−44.
(56) Claussen, J. C.; Kim, S. S.; Haque, A. ul; Artiles, M. S.; Porterfield, D. M.; Fisher, T. S. Electrochemical Glucose Biosensor of Platinum Nanospheres Connected by Carbon Nanotubes. *J. Diabetes Sci. Technol.* **2010**, *4*, 312−319.